Polymer Journal (2011) 43, 849–854

www.nature.com/pj

ORIGINAL ARTICLE

Directional electromechanical properties of PEDOT/PSS films containing aligned electrospun nanofibers

Jian Zhou, Tadashi Fukawa and Mutsumi Kimura

We demonstrate directional electromechanical properties of poly(3,4-ethylenedioxythiophene)/poly(4-styrene sulfonate) (PEDOT/PSS) composite films containing aligned poly(vinyl pyrrolidone)/poly(methyl methacrylate) nanofiber assemblies. The aligned nanofiber assemblies showed anisotropic wettability based on the high alignment degree of the nanofibers. The PEDOT/PSS composite film containing aligned nanofibers displayed an anisotropic actuation response when a voltage was applied in air. The orientation of the embedded nanofibers within the PEDOT/PSS matrix leads to the control of actuation direction because of the difference of anisotropic mechanical properties in the composite films.
Polymer Journal (2011) **43,** 849–854; doi:10.1038/pj.2011.62; published online 27 July 2011

Keywords: anisotropic actuation; conductive polymer; electrospinning; mechanical properties; wetting

INTRODUCTION

Living things have acquired special anisotropic functions based on directional orientations of micro- and nanostructures during their evolution. Anisotropic structures in nature make possible directional motion, adhesion, friction or wetting.[1–4] These natural structures provide important insights for constructing artificial materials. Thus, bio-inspired advanced materials have been developed to mimic natural anisotropic structures.[5–9]

Long, fibrous structures, such as collagens and celluloses, are a major component of the extracellular matrix that supports most tissues by maintaining their strength and elasticity.[10] Moreover, composite materials with incorporated highly dense fibrous assemblies have been widely developed, and these materials show significantly different physical and chemical properties, which remain separate and distinct at the macroscopic or microscopic scale within the finished structure.[11,12] Fiber orientation within natural and artificial composites is a key factor in determining final properties. Several anisotropic functions of aligned nanofiber assemblies have been reported in the literature. Vertically aligned multiwalled carbon nanotube assemblies show strong adhesion to vertical surfaces, similar to gecko legs.[13] Anisotropic hydrophobic properties have been demonstrated by aligned nanofiber assemblies.[14] In this study, we focus on control of electromechanical properties of conjugated polymer films by using aligned electrospun nanofiber assemblies.

Electrospinning is a simple method for producing nanofibers and nanofibrous non-woven mats for various applications. It involves discharging a polymer solution in air from a nozzle under high voltage and producing nanofibers by exploiting electrostatic repulsion of the polymer solution.[15–17] Furthermore, the fiber orientation can be controlled by using modified fiber collectors.[18] Aligned electrospun nanofibers have potential applications in structural reinforcement, tissue engineering and blood vessel engineering, which often require well-aligned and highly ordered structures.[16,17] There are only a few reports in the literature on anisotropic actuation based on anisotropic structures. Anisotropic actuation of polypyrrole films was achieved by orientation of polymer backbones through directional stretching.[19] Uniaxial orientation of nafion, and the subsequent formation of electrode layers to create ionic polymer–metal composites, can also yield anisotropic actuation on electrical stimulation.[20]

As the application of fiber-reinforced composite becomes more widespread, there is a desire to add functionality not only simple enhancement of mechanical properties but also development of smart materials. Bent[21] reported that the active fibers composites, which incorporated unidirectional piezoelectric transducer fibers into hybrid matrix, produce a highly conformable and anisotropic actuator material. We also reported anisotropic actuation of poly (3, 4-ethylenedioxythiophene)/poly(4-styrene sulfonate) (PEDOT/PSS) coated papers, for which the actuation stress depended on the relative orientation of paper fibers and the loading direction of the coating.[22] When the aligned nanofiber assemblies were embedded within the conductive polymer matrix, the actuation properties followed the direction of fiber orientation. In this study, we selected aligned electrospun nanofibers for anisotropic actuation of conductive polymers. We fabricated aligned poly(vinyl pyrrolidone)/poly(methyl methacrylate) (PVP/PMMA) nanofiber assemblies up to several centimeters in length to realize anisotropic motion of PEDOT/PSS

Department of Functional Polymer Science, Faculty of Textile Science and Technology, Shinshu University, Ueda, Japan
Correspondence: Professor M Kimura, Department of Functional Polymer Science, Faculty of Textile Science and Technology, Shinshu University, Ueda 386-8567, Japan.
E-mail: mkimura@shinshu-u.ac.jp
Received 8 April 2011; revised 24 May 2011; accepted 30 May 2011; published online 27 July 2011

films. The aligned nanofiber assemblies displayed anisotropic wettability because of the high alignment degree of the nanofibers. We further demonstrated anisotropic electromechanical actuation of PEDOT/PSS film by using the aligned PVP/PMMA nanofibers. The composites with incorporated aligned nanofiber assemblies offer new opportunities to achieve directional electromechanical actuation in soft actuators.

EXPERIMENTAL PROCEDURE

Materials

Poly(vinylpyrrolidone) (PVP, Nacalai Tesque, Tokyo, Japan, Mw 1 000 000 g mol^{-1}), poly(methyl methacrylate) (PMMA, Wako Chemicals, Tokyo, Japan, Mw 100 000 g mol^{-1}), ethylene glycol (EG, Wako Chemicals), *N*,*N*-dimethylformamide (Wako Chemicals), tetra-*n*-butylammonium bromide (Wako Chemicals) and fuchsine (Wako Chemicals) were used as received. Poly(vinyl alcohol) (Mw 140 000 g mol^{-1}) was provided by Kuraray Co., Ltd (Tokyo, Japan).

Fabrication of nanofiber assemblies by electrospinning

Nanofiber assemblies were fabricated using a NANON-01A electrospinning machine with a drum collector (MECC Co., Ltd, Fukuoka, Japan). PVP/PMMA nanofiber assemblies were produced from 250 mg ml^{-1} PVP and PMMA in a *N*,*N*-dimethylformamide solution containing 5 wt% tetra-*n*-butylammonium bromide (relative to PMMA).[22,23] The mixed solutions for the PVP/PMMA composite nanofibers were prepared by dissolving PVP and PMMA (weight ratio PVP: PMMA=10:90) in *N*,*N*-dimethylformamide. Tetra-*n*-butylammonium bromide was used as an organic salt to increase the electrical conductivity of the solution.[24] In the electrospinning process, the prepared solutions were placed in 6 ml disposable plastic syringes and injected through a stainless steel needle (18 gauge, orifice diameter 1.2 mm). The needle was connected to a high-voltage direct current power supply. The solutions were continuously fed by a syringe pump through the nozzle at a rate of 0.4 ml h^{-1}. A high voltage (14 kV) and a distance of 14 cm between the needle and the drum collector were used. The drum collector, which was connected with the ground and used as a target electrode, was rotated at 50 and 3000 r.p.m. min^{-1} to collect non-aligned and aligned nanofiber assemblies, respectively.[18] The relative humidity in the chamber was maintained at about 35% by flowing N_2.

Dynamic contact angle measurement

For each experiment, fuchsine solution at a concentration of 1×10^{-5} M was used instead of deionized water to ensure a clear view of droplets. A 0.5-μl droplet was deposited using a micropipette on the surfaces of nanofiber assemblies. Images of the spreading of the droplet were recorded using both a top view KH-7700 digital microscope with an AD-5040 L macrolens (Hirox Co., Ltd, Tokyo, Japan) and a side view IUC200-CK2 camera (Trinity Co., Ltd) at a frame rate of 30 f.p.s. The dynamic contact angle and base diameter were determined with the side view camera. A minimum of 10 drops were examined for each surface.[7]

Deposition of PEDOT/PSS dispersion on PVP/PMMA nanofiber assemblies

The weights of non-aligned and aligned PVP/PMMA nanofiber mats were 25.4 mg and 24.4 mg, respectively, with area 4×7 cm. Each nanofiber mat was placed on a polyethylene (PE) film and well-dispersed PEDOT/PSS aqueous dispersion (1.3 wt% solid content, 2.0 g) containing 5 wt% EG was deposited on the nanofiber mat, then the sample was dried at 100 °C for 2 h. EG was used as an additive to enhance the electronic conductivity of PEDOT/PSS.

Measurements

Morphologies of nanofibers were examined with a VE-8800SP (Keithley Co., Ltd.) scanning electronic microscope (SEM). The angle distribution of the nanofibers was determined from the SEM images using image tools. The nanofiber alignment was quantified by measuring the angles between the desired direction and the longitudinal axes of the nanofibers. A total of 200 fibers were examined from SEM images over an area of 0.18×0.25 mm^2 for each nanofiber mat. The orientation parameter that was originally suggested in the field of fiber composites was adapted to quantitative analysis of the electrospun nanofibers.[24,25] Mechanical properties were evaluated with a RTC-1250A tension tester (A&D Co., Ltd, Tokyo, Japan) at a constant strain rate of 100% min^{-1} (chuck distance 30 mm). Tensile specimens were prepared with length 30 mm. Young's modulus, tensile strength and elongation at break were calculated from the stress-strain curves as average values from at least five determinations.

The electromechanical properties of PEDOT/PSS films were tested with a ZP-2N force gauge (Imada Co., Ltd, Nagoya, Japan). A composite film specimen with size 40×3 mm was placed in a humidity-controlled chamber. An electric field was applied to the film by a computer-driven PK-80 DC power supply (Matsusada Co., Ltd, Kusatsu, Japan) through a pair of copper wires (170 mm) attached to the PEDOT/PSS film with silver paste; the distance between the electrodes was about 30 mm. The electric currents were monitored with a U1252A digital multimeter (Agilent Co., Ltd, Tokyo, Japan).

RESULTS AND DISCUSSION

Aligned electrospun nanofiber assemblies were prepared from 250 mg ml^{-1} PVP/PMMA (weight ratio 10/90) in *N*,*N*-dimethylformamide containing 5 wt% tetra-*n*-butylammonium bromide with respect to PMMA.[23,24] Electrospun nanofibers were collected on the drum collector rotated at 3000 r.p.m. The SEM image of aligned PVP/PMMA nanofiber assemblies shows that nanofibers with average diameter 342 ± 56 nm were well arranged and formed a dense array (Figure 1a). The thickness of the aligned nanofiber assembly used in this study was approximately 22 μm. Although substantial misalign-

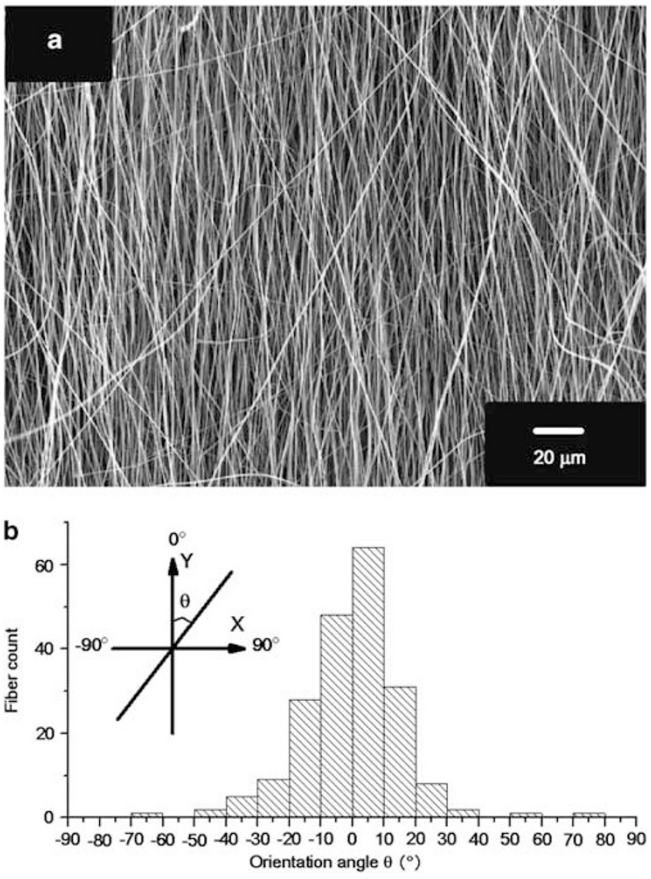

Figure 1 (**a**) Scanning electronic microscope image of aligned poly(vinyl pyrrolidone)/poly(methyl methacrylate) nanofiber assemblies. (**b**) Histogram of orientation distribution of the poly(vinyl pyrrolidone)/poly(methyl methacrylate) nanofibers.

ment was still observed in the fiber assemblies, it was found that at least 85.5% of the nanofibers were oriented within $\pm 20^{\circ}$ of the preferred direction (Figure 1b). The orientation parameter of the nanofiber assembly was estimated to be 0.86 by statistical analysis of the direction histogram.[25,26] The value obtained is comparable with the reported value for electrospun poly(ethylene oxide) nanofiber assemblies collected at 2500 r.p.m.[26,27] Non-aligned nanofiber mats were prepared at drum rotation speed of 50 r.p.m. min^{-1} using the same mother solution of PVP/PMMA. The orientation parameter of the non-aligned fiber mat was determined to be 0.08 (Supplementary Figure S1).

The wettability of these nanofiber assemblies is a key attribute for coating the polymer matrix. During the coating process, polymer solution penetrated into the nanofiber assemblies and covered all surfaces of the nanofibers. A 0.5 µl water droplet spread on the non-aligned nanofiber mat formed a spherical shape and displayed complete isotropic wetting after 4 s. However, the same droplet on aligned nanofiber assemblies showed anisotropic wetting similar to the behavior of a water droplet on grooved surfaces.[5,28,29] Figure 2 shows the time-course of water droplet deformation on the aligned nanofiber assemblies. The *x*- and *y*-directions in Figure 2 show the directions of movement of the droplet as parallel and perpendicular to the oriented nanofibers (subscripts for θ_x and θ_y mean the observation direction). Although the contact angle measured in the *x*-direction θ_x was 128°, the contact angle θ_y was found to be 98°. Both angles were significantly larger than the contact angle for a PVP/PMMA solution cast film (51°). The nanofiber assemblies include the effect of microscopic air pockets trapped below the liquid droplet, which leads to a hydrophobic interface.[30,31] The addition of water-soluble PVP to PMMA changed the wettability of the nanofiber assemblies by reducing surface energy while maintaining the fibrous morphology. The contact angles in both directions approached zero by penetration of the water droplet into the nanofiber matrix. In comparison, the contact angles of water on the PMMA nanofiber assemblies in both directions are over 115° (144° and 115°). The water droplet set on PMMA nanofiber assemblies with air pockets below, which prevented water from contacting the PMMA surface completely by trapping air at the water–PMMA nanofiber interface. Time-lapse images of a liquid droplet spreading on aligned PVP/PMMA fiber mat are shown in Figures 2b and c. The initially spherical droplet spread on the aligned PVP/PMMA nanofiber assemblies, and was deformed into an ellipsoidal shape. Finally, the droplet penetrated into the nanofiber matrix and achieved complete wetting after 180 s.

To confirm the role of the contact line pinning of aligned nanofiber assemblies in determining the droplet shape, the dynamic contact angles and base diameter both perpendicular and parallel to the *y*-axis were measured as a function of time. Figure 3 shows the time-courses of the contact angles and base diameters of a water droplet on aligned and non-aligned nanofiber assemblies. The dynamic contact angles and the base diameters in both directions on a non-aligned nanofiber mat decreased within 4 s. The profiles in the *x*-axis were comparable with those in the *y*-axis. By contrast, the aligned nanofiber assemblies required 180 and 100 s, following attainment of the equilibrium contact angles θ_x and θ_y, to reach complete wetting (Figures 3a and b). On the aligned nanofiber assemblies, the base diameter d_x increased gradually for 100 s then became constant, whereas the base diameter d_y was roughly constant during the experiment (Figures 3c and d). The final drop elongation, calculated from the diameter ratios in the *x*- and *y*-directions of the ellipsoidal droplet on the aligned nanofiber assembly, was 2.5, whereas for the drop on the non-aligned nanofiber mat the elongation was 1.0 (Figures 3c and d). Thus, the non-aligned nanofiber mat exhibited isotropic spreading of the droplet and there were no pinning barriers for contact line motion. On the other hand, the aligned nanofiber assembly showed directional spreading of the droplet along the alignment direction of the nanofibers. These results clearly confirmed that the aligned nanofiber assemblies had a high degree of alignment while maintaining their wettability.

Electro-active PEDOT/PSS films have been found to exhibit excellent isotropic actuation properties as a result of controlling the water vapor sorption equilibrium in response to an electric field.[22,32] The electromechanical properties are affected by ambient humidity that changes water uptake of the PEDOT/PSS film or PEDOT/PSS coated papers.[32,33] When the aligned nanofiber assemblies were embedded in the PEDOT/PSS matrix, the anisotropic structure affected the directional actuation of the composite. The procedure for fabrication of aligned nanofiber-embedded PEDOT/PSS composite is shown schematically in Figure 4a. PEDOT/PSS aqueous dispersion

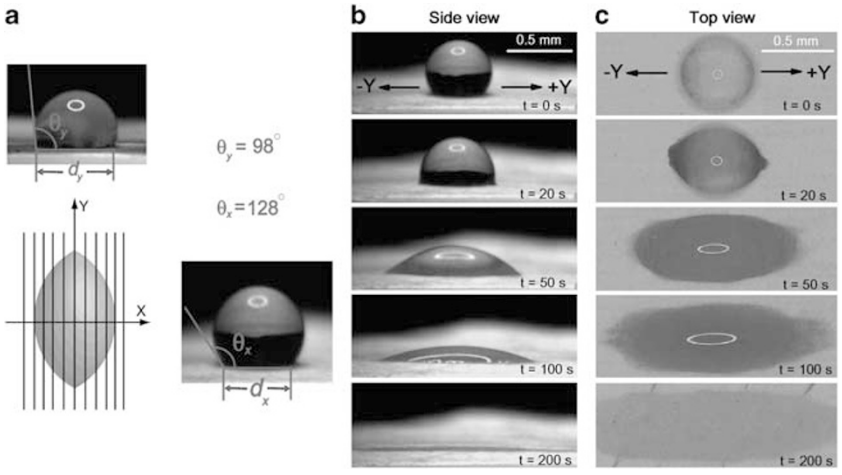

Figure 2 (**a**) Illustration for the directional measurement of contact angles on aligned poly(vinyl pyrrolidone)/poly(methyl methacrylate) fibers, subscripts for θ_x and θ_y mean the observation direction. (**b**, **c**) Time-lapse images of liquid droplet spreading on poly(vinyl pyrrolidone)/poly(methyl methacrylate) fiber mat: **b**, side view and **c**, top view. A 0.5-µl water droplet (fuchsine concentration: 1×10^{-5} M) was spread on aligned poly(vinyl pyrrolidone)/poly(methyl methacrylate) nanofiber assemblies. The drop motions are highlighted by the arrows in **b** and **c**. A full color version of this figure is available at *Polymer Journal* online.

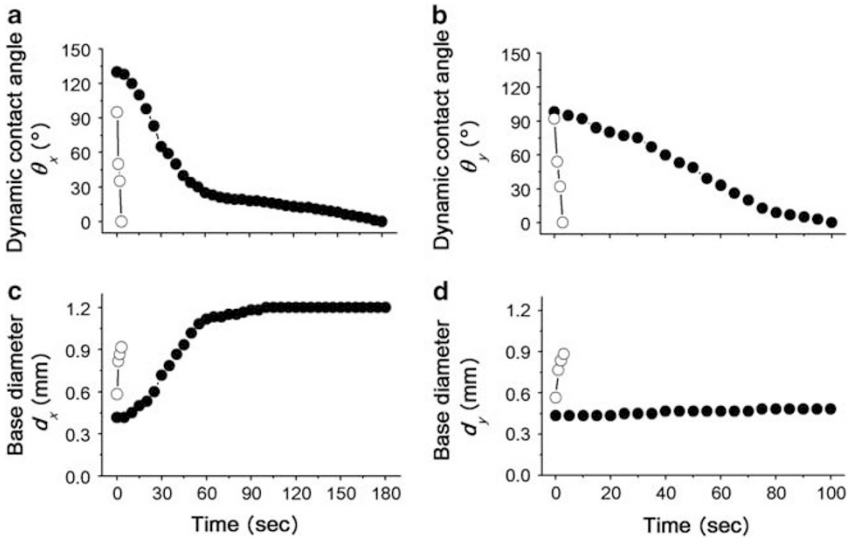

Figure 3 (**a**, **b**) Dynamic contact angle parallel and perpendicular to the *y*-axis (see the definition in Figure 2a) as a function of time for poly (vinyl pyrrolidone)/poly(methyl methacrylate) nanofiber mat. (**c**, **d**) Base diameter perpendicular and parallel to the *y*-axis as a function of time for poly (vinyl pyrrolidone)/poly(methyl methacrylate) nanofiber assemblies (●) and no-naligned nanofiber mat (○), subscripts for d_x and d_y mean the observation direction.

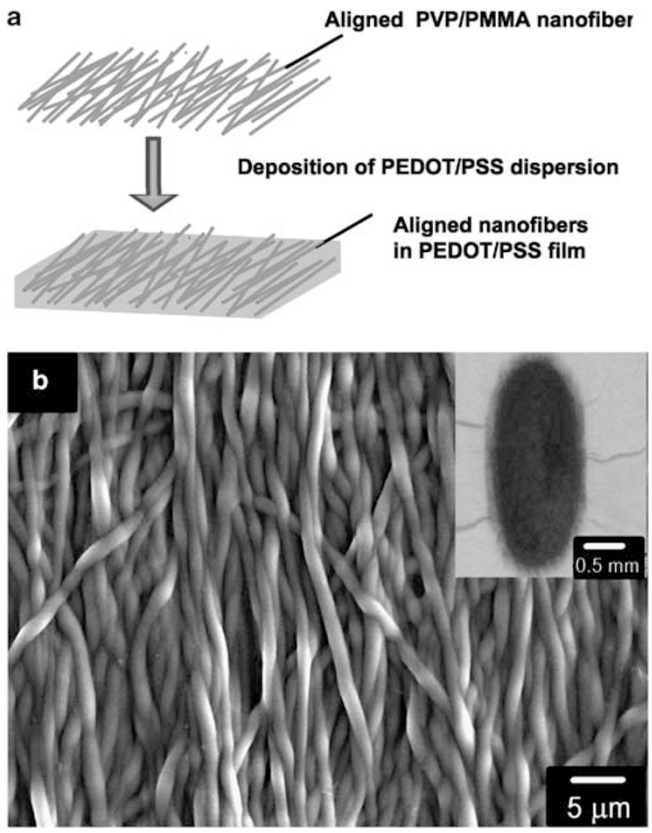

Figure 4 (**a**) Schematic illustration of the preparation of poly(3,4-ethylenedioxythiophene)/poly(4-styrene sulfonate) (PEDOT/PSS) composite film containing aligned nanofiber assemblies. (**b**) Scanning electronic microscope image of the surface of PEDOT/PSS composite film containing aligned poly(vinyl pyrrolidone)/poly(methyl methacrylate) (PVP/PMMA) nanofibers. Inset is optical image of PEDOT/PSS dispersion wetted spot on aligned nanofiber assemblies. A full color version of this figure is available at *Polymer Journal* online.

displayed complete wetting similar to water on the aligned nanofiber assemblies. It easily penetrated into the aligned nanofiber assemblies and wetted all surfaces of the nanofibers. Figure 4b shows an SEM image of the PEDOT/PSS film containing the aligned PVP/PMMA nanofiber mat, showing aligned fibrous morphology after coating. A PEDOT/PSS layer was coated on the surfaces of the aligned nanofibers, and the interspace between nanofibers was filled with PEDOT/PSS. The contour of a PEDOT/PSS wetted spot revealed an elongated and parallel-sided shape (inset to Figure 4b) with elongation value of 2.1. This shape is typically observed on grooved surfaces, which again confirms that the nanofibers were highly orientated.[5,28,29] The orientation parameter of the coated nanofibers was determined as 0.82 (Supplementary Figure S2), in agreement with the value for uncoated aligned nanofibers. Inside the PEDOT/PSS layer, the aligned nanofibers were fully covered with PEDOT/PSS (Supplementary Figure S3). It should be pointed out that the sheet resistance of this PEDOT/PSS film without EG is 1.6 kΩ per square. By mixing with 5% of EG, the sheet resistance can be reduced to a low level of 5.7 Ω per square corresponding to a conductivity of 150 S cm^{-1} in the PEDOT/PSS film. The enhancement in conductivity was caused by the benzoid structure of PEDOT transforming into a quinoid structure.[34–36]

Young's modulus of the aligned nanofiber-embedded PEDOT/PSS composite film along the nanofiber orientation direction was 2.2 ± 0.2 GPa, nearly three times that of non-aligned nanofibers (0.8 ± 0.1 GPa). Moreover, this value was almost five times the value perpendicular to the nanofiber direction, showing the anisotropic mechanical properties of the composite film (Figure 5a).

The electromechanical properties of PEDOT/PSS composite films with incorporated aligned nanofiber assemblies were investigated by the stress generation by applying a voltage. Figures 5b and c show the time profiles of the generated stress and current for three different PEDOT/PSS films at 50% relative humidity and 25 °C. When a voltage of 2.8 V was applied to the PEDOT/PSS composite film, the film generated a large stress in response to the electric field. Turning off the applied voltage returned the stress to zero. The currents for the three samples were almost the same at about 53 mA at 2.8 V applied voltage.

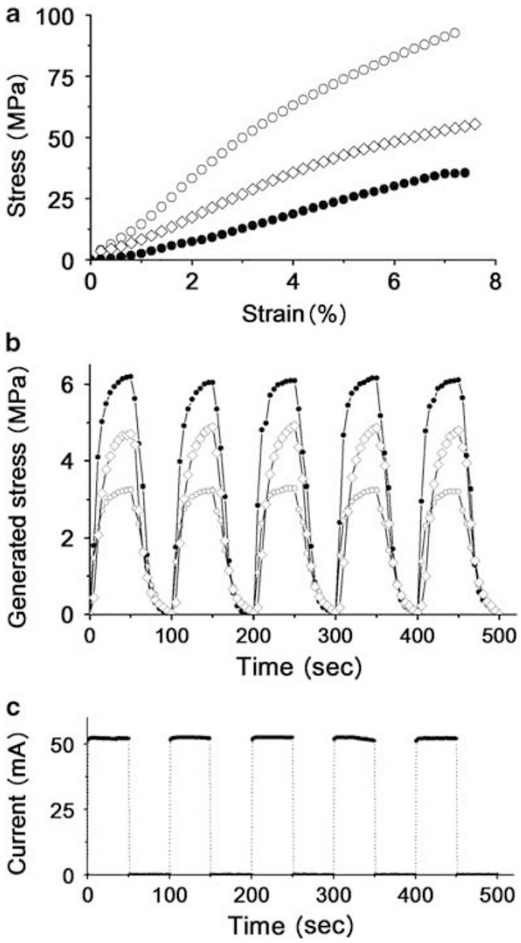

Figure 5 (**a**) Stress-strain curves of poly(3,4-ethylenedioxythiophene)/poly(4-styrene sulfonate) composite films with non-aligned and aligned nanofibers and (**b**) time profiles of the generated stress of loading direction parallel to aligned nanofiber direction (○), loading direction perpendicular to aligned nanofiber direction (●) of poly(3,4-ethylenedioxythiophene)/poly(4-styrene sulfonate) composite films with aligned nanofiber assemblies and poly(3,4-ethylenedioxythiophene)/poly(4-styrene sulfonate) film with non-aligned nanofiber mat (◇). (**c**) Time profile of the current of poly (3,4-ethylenedioxythiophene)/poly(4-styrene sulfonate) composite films at 25ºC with 50% relative humidity.

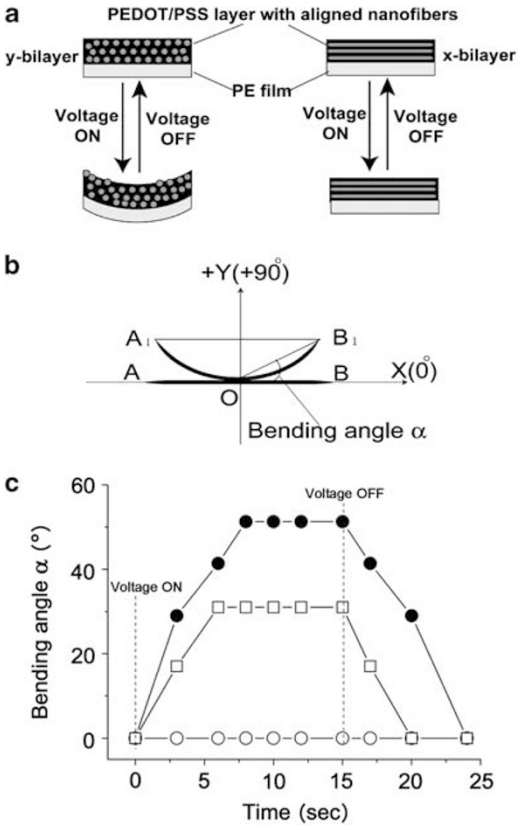

Figure 6 (**a**) Illustration of poly(3,4-ethylenedioxythiophene)/poly(4-styrene sulfonate (PEDOT/PSS)–polyethylene (PE) bilayer with aligned nanofiber assemblies. Left image: y-bilayer, right image: x-bilayer. (**b**) Schematic illustration of the bending/unbending motions. (**c**) Time-dependent bending angles of PEDOT/PSS–PE bilayer with aligned nanofiber assemblies (●, y-bilayer; ○, x-bilayer) and PEDOT/PSS–PE bilayer with non-aligned nanofiber mat (□). The bending actuations are measured under an applied constant current of 53 mA at 25 °C with 50% relative humidity. A full color version of this figure is available at *Polymer Journal* online.

However, the stress generated along the nanofiber direction was 3.2 MPa, and only 50% of the stress perpendicular to the nanofiber direction. The PEDOT/PSS film containing the non-aligned nanofiber mat showed an intermediate stress of 4.7 MPa. We propose that this anisotropic electromechanical actuation can be attributed to the anisotropic mechanical properties of the PEDOT/PSS composite film containing aligned nanofiber assemblies. The stress that is generated depends strongly on the orientation angle of the nanofibers within the composite films.

Bilayer actuators were fabricated by deposition of PEDOT/PSS composite film onto PE thin film in the same manner that PEDOT/PSS composite film was made. Poly(vinyl alcohol) was used as an adhesion interlayer between PE and the PVP/PMMA nanofiber mat to prevent the PEDOT/PSS film from peeling off. The thicknesses of PE film, poly(vinyl alcohol) interlayer and PEDOT/PSS composite film were 10 μm, 0.55 μm and 27 μm, respectively. Two PEDOT/PSS–PE bilayers containing the aligned nanofiber assemblies were prepared by cutting the bilayer in two directions. Cross-sectional images of the bilayer actuators are depicted in Figure 6a. The left image shows the aligned nanofiber direction parallel to the loading direction, and is defined as a y-bilayer. The right image shows the aligned nanofiber direction perpendicular to the loading direction, and is defined as an x-bilayer. The y-bilayer displayed a bending/unbending motion in response to an applied voltage of 2.8 V, whereas no obvious motion of the x-bilayer was observed. Figure 6b shows a schematic illustration of the bending/unbending movement of the bilayer actuators. The bending angle (α) of the bilayer actuator was obtained from the width between the two positions A_1 and B_1. Figure 6c shows the time-dependent bending angles of the PEDOT/PSS–PE bilayer. The PEDOT/PSS composite layer on the PE film shrunk by applying a voltage because of the water vapor desorption from the electro-active PEDOT/PSS, and the bilayer bent as the result of shrinking of the PEDOT/PSS layer. The y-bilayer bent from 0 to 53° within 8 s of after applying the electrical field, indicating a bending speed of $7.9\,^{\circ}\,s^{-1}$. However, the x-bilayer showed no motion on application of the same voltage. Thus, the PEDOT/PSS–PE bilayer with incorporated non-aligned nanofiber mat showed an isotropic bending motion on application of the electrical field. It follows that the bending motion is affected by the alignment of the nanofiber structures in the PEDOT/PSS layer, and the difference of Young's modulus in the composite films results in the anisotropic bending actuation.

Conclusions

Anisotropic actuation properties using electrospun nanofiber assemblies can be obtained by controlling the alignment of the nanofibers and fully covering the nanofibers with electro-active conductive polymers. The orientation of the nanofibers pre-determined an anisotropic generating stress and bending motion. Aligned nanofiber assemblies were prepared by collection of electrospun nanofibers on a rotating drum collector. The alignment of nanofiber assemblies was evaluated by statistical analysis of the nanofiber direction histogram and anisotropic wettability. PEDOT/PSS composite film incorporating the aligned nanofiber assemblies exhibited anisotropic electromechanical properties due to the anisotropic mechanical properties within the composite film. This study will open prospects for the construction of anisotropic actuators based on directional orientation of nanofibers, and further investigation may lead to fabrication of low-cost, flexible ambient devices with anisotropic actuation properties.

ACKNOWLEDGEMENTS

This work was partially supported by the Global COE Program for 'International Center of Excellence on Fiber Engineering' and Knowledge Cluster Initiative Program (Second Stage) 'Shinshu Smart Devices Cluster' from the Ministry of Education, Culture, Sports, Science and Technology, Japan.

1 Autumn, K., Sitti, M., Ling, Y. A., Peattie, A. M., Hansen, W. R., Sponberg, S., Keny, T. W., Fearing, R., Israelachvili, J. N. & Full, R. J. Evidence for Van Der Waals adhesion in Gecko Setae. *Proc. Natl. Aca. Sci.* **99,** 12252–12256 (2002).
2 Whitney, H. M., Kolle, M., Andrew, P., Chittka, L., Steiner, U. & Glover, B. J. Floral iridescence, produced by diffractive optics, acts as a cue for animal pollinators. *Science* **323,** 130–133 (2009).
3 Zheng, Y. M., Gao, X. F. & Jiang, L. Directional adhesion of superhydrophobic butterfly wings. *Soft Matter* **3,** 178–182 (2007).
4 Binzoni, T., Courvoisier, C., Giust, R., Tribillon, G., Gharbi, T., Hebden, J. C., Leung, T. S., Roux, J. & Delpy, D. T. Anisotropic photon migration in human skeletal muscle. *Phys. Med. Biol.* **51,** 79–90 (2006).
5 Xia, D. Y. & Brueck, S. R. J. Strongly anisotropic wetting on one-dimensional nanopatterned surfaces. *Nano Lett.* **8,** 2819–2824 (2008).
6 Malvadkar, N. A., Hancock, M. J., Sekeroglu, K., Dressick, W. J. & Demirel, M. C. An engineered anisotropic nanofilm with unidirectional wetting properties. *Nat. Mater.* **9,** 1023–1028 (2010).
7 Chu, K. H., Xiao, R. & Wang, E. N. Unidirectional liquid spreading on asymmetric nanostructured surfaces. *Nat. Mater.* **9,** 413–417 (2010).
8 Chung, J. Y., Youngblood, J. P. & Stafford, C. M. Anisotropic wetting on tunable micro-wrinkled surfaces. *Soft Mater* **3,** 1163–1169 (2007).
9 Wu, D., Chen, Q. D., Yao, J., Guan, Y. C., Wang, J. N., Niu, L. G., Fang, H. H. & Sun, H. B. A simple strategy to realize biomimetic surfaces with controlled anisotropic wetting. *Appl. Phys. Lett.* **96,** 0537041–0537043 (2010).
10 Fratzl, P. Cellulose and collagen: from fibers to tissues. *Curr. Opin. Coll. Interface. Sci.* **8,** 32–39 (2003).
11 Dryden, J., Deakin, A. & Zok, F. Effect of cracks on the thermal resistance of aligned fiber composites. *J. Appl. Phys.* **92,** 1137–1142 (2002).
12 Gu, B. K., Ismail, Y. A., Spinks, G. M., Kim, S. I., So, I. & Kim, S. J. A linear actuation of polymeric nanofibrous bundle for artificial muscles. *Chem. Mater.* **21,** 511–515 (2009).
13 Qu, L. T., Dai, L. M., Stone, M., Xia, Z. H. & Wang, Z. L. Carbon nanotube arrays with strong shear binding-on and easy normal lifting-off. *Science* **322,** 238–242 (2008).
14 Wu, H., Zhang, R., Sun, Y., Lin, D. L., Sun, Z. Q., Pan, W. & Downs, P. Biomimetic nanofiber patterns with controlled wettability. *Soft Matter* **4,** 2429–2433 (2008).
15 Dzenis, Y. Spinning continuous fibers for nanotechnology. *Science* **304,** 1917–242 (2004).
16 Greiner, A. & Wendorff, J. H. Electrospinning: a fascinating method for the preparation of ultrathin fibers. *Angew. Chem. Int. Ed.* **46,** 5670–5703 (2007).
17 Xie, J. W., Li, X. R. & Xia, Y. N. Putting electrospun nanofibers to work for biomedical research. *Macromol. Rapid Commun.* **29,** 1775–1792 (2008).
18 Katta, P., Alessandro, M., Ramsier, R. D. & Chase, G. G. Continuous electrospinning of aligned polymer nanofibers onto a wire drum collector. *Nano Lett.* **4,** 2215–2218 (2004).
19 Pytel, R., Thomas, E. & Hunter, I. Anisotropy of electroactive strain in highly stretched polypyrrole actuator. *Chem. Mater.* **18,** 861–863 (2006).
20 Park, J. K. & Moore, R. B. Influence of ordered morphology on the anisotropic actuation in uniaxially oriented electroactive polymer systems. *ACS App. Mater. Interfaces* **1,** 697–702 (2009).
21 Bent, A. A. Active fiber composite material systems for structural control applications. *Proceeding of SPIE Conference on Industrial and Commercial Applications of Smart Structures* **3674,** 166–176 (1999).
22 Zhou, J., Fukawa, T., Shirai, H. & Kimura, M. Anisotropic motion of electroactive papers coated with PEDOT/PSS. *Macromol. Mater. Eng.* **295,** 671–675 (2010).
23 Dong, H. & Jones, W. E. Jr. Preparation of submicron polypyrrole/poly (methyl methacrylate) coaxial fibers and conversion to polypyrrole tubes and carbon tubes. *Langmuir* **22,** 11384–11387 (2006).
24 Dong, H., Nyame, V., Macdiarmid, A. G. & Jones, W. E. Polyaniline/poly(methyl methacrylate) coaxial fibers: the fabrication and effects of the solution properties on the morphology of electrospun core fibers. *J. Polym. Sci. Part B: Polym. Phys.* **42,** 3934–3942 (2004).
25 Gadala-Maria, F. & Parsi, F. Measurement of fiber orientation in short-fiber composites using digital image processing. *Polym. Composite* **14,** 126–131 (1993).
26 Liu, L. & Dzenis, Y. A. Analysis of effects of the residual charge and gap size on electrospun nanofiber alignment in a gap method. *Nanotechnology* **19,** 1–7 (2008).
27 Park, S. H. & Yang, D. Y. Fabrication of aligned electrospun nanofibers by inclined gap method. *J. Appl. Polym. Sci.* **120,** 1800–1807 (2011).
28 Kusumastmaja, H., Vrancken, R. J., Bastiaansen, C. W. M. & Yeomans, J. M. Anisotropic drop morphologies on corrugated surfaces. *Langmuir* **24,** 7299–7308 (2008).
29 Yang, J., Rose, F.R.A.J., Gadegaard, N. & Alexander, M. R. Effect of sessile drop volume on the wetting anisotropy observed on grooved surfaces. *Langmuir* **25,** 2567–2571 (2009).
30 Lafuma, A. & Quéré, D. Superhydrophobic states. *Nat. Mater.* **2,** 457–460 (2003).
31 Tuteja, A., Choi, W., Ma, M. L., Mabry, J. M., Mazzella, S. A., Rutledge, G. C., McKinley, G. H. & Cohen, R. E. Designing superroleophobic surfaces. *Science* **318,** 1618–1622 (2007).
32 Okuzaki, H., Suzuki, H. & Ito, T. Electromechanical properties of poly(3, 4-ethylenedioxythiopene)/poly(4-styrene sulfonate). *J. Phys. Chem. B* **113,** 11378–11383 (2009).
33 Zhou, J., Gao, Q., Fukawa, T., Shirai, H. & Kimura, M. Macroporous conductive polymer films fabricated by electrospun nanofiber templates and their electromechanical properties. *Nanotechnology* **22,** 275501 (2011).
34 Huang, J., Miller, P. F., Wilson, J. S., De Mello, J. C., De Mello, A. J. & Bradley, D. C. Investigation of the effects of doping and post-deposition treatment on the conductivity, morphology, and work function of poly (3, 4-ethylenedioxythiophene): poly (styrene sulfonate) films. *Adv. Funct. Mater.* **15,** 290–296 (2005).
35 Hsiao, Y. S., Whang, W. T., Chen, C. P. & Chen, Y. C. High-conductivity poly (3, 4-ethylenedioxythiophene): poly (styrene sulfonate) film for use in ITO-free polymer solar cells. *J. Mater. Chem.* **18,** 5948–5955 (2008).
36 Xia, Y. J. & Ouyang, J. Y. Significant conductivity enhancement of conductive poly(3,4-ethylenedioxythiophene): poly(styrenesulfonate) films through a treatment with organic carboxylic acids and inorganic acids. *ACS Appl. Mater. Interfaces* **2,** 474–483 (2010).

Supplementary Information accompanies the paper on Polymer Journal website (http://www.nature.com/pj)